AMERICAN SOCIETY FOR MICROBIOLOGY | Journal of Virology®

PATHOGENESIS AND IMMUNITY

# Dok-1 and Dok-2 Are Required To Maintain Herpes Simplex Virus 1-Specific CD8$^+$ T Cells in a Murine Model of Ocular Infection

**Soumia Lahmidi, Mitra Yousefi,* Slimane Dridi, Pascale Duplay, Angela Pearson**

INRS-Institut Armand-Frappier, Laval, Québec, Canada

**ABSTRACT** Dok-1 and Dok-2 negatively regulate responses downstream of several immune receptors in lymphoid and myeloid cells. Recent evidence showed that Dok proteins are essential in the formation of memory CD8$^+$ T cells to an exogenous epitope expressed by vaccinia virus; however, the importance of Dok-1 and Dok-2 in the control of viral infection is unknown. Here, we investigated the role of Dok proteins in modulating the immune response against herpes simplex virus 1 (HSV-1) in a mouse model of ocular infection. During acute infection, viral titers in the eye were similar in wild-type (WT) and Dok-1 and Dok-2 double-knockout (DKO) mice, and the percentages of infiltrating leukocytes were similar in DKO and WT corneas and trigeminal ganglia (TG). DKO mice exhibited a diminished CD8$^+$ T cell response to the immunodominant HSV-1 glycoprotein B (gB) epitope in the spleen and draining lymph nodes compared to WT mice during acute infection. Remarkably, gB-specific CD8$^+$ T cells almost completely disappeared in the spleens of DKO mice during latency, and the reduction of CD8$^+$ effector memory T (Tem) cells was more severe than that of CD8$^+$ central memory T (Tcm) cells. The percentage of gB-specific CD8$^+$ T cells in TG during latency was also dramatically reduced in DKO mice; however, they were phenotypically similar to those from WT mice. In *ex vivo* assays, reactivation was detected earlier in TG cultures from infected DKO versus WT mice. Thus, Dok-1 and Dok-2 promote survival of gB-specific CD8$^+$ T cells in TG latently infected with HSV-1.

**IMPORTANCE** HSV-1 establishes lifelong latency in sensory neurons of trigeminal ganglia (TG). In humans, HSV-1 is able to sporadically reactivate from latently infected neurons and establish a lytic infection at a site to which the neurons project. Most herpetic disease in humans is due to reactivation of HSV-1 from latency rather than to primary acute infection. CD8$^+$ T cells are thought to play an important role in controlling recurrent infections. In this study, we examined the involvement of Dok-1 and Dok-2 signaling proteins in the control of HSV-1 infection. We provide evidence that Dok proteins are required to maintain a CD8$^+$ T cell response against HSV-1 during latency—especially CD8$^+$ Tem cells—and that they negatively affect HSV-1 reactivation from latency. Elucidating Dok-mediated mechanisms involved in the control of HSV-1 reactivation from latency might contribute to the development of therapeutic strategies to prevent recurrent HSV-1-induced pathology.

**KEYWORDS** CD8$^+$ T cell, T cell immunity, Dok proteins, herpes simplex virus, herpesviruses, viral pathogenesis

Following experimental corneal infection of C57BL/6 (B6) mice, herpes simplex virus 1 (HSV-1) replicates in epithelial cells and then spreads to the trigeminal ganglia (TG) via nerve termini, where it replicates but then ultimately establishes latency in neurons (1). In humans, reactivation of HSV-1 can lead to recurrent lesions on labial

**Received** 30 November 2016 **Accepted** 2 May 2017

**Accepted manuscript posted online** 10 May 2017

**Citation** Lahmidi S, Yousefi M, Dridi S, Duplay P, Pearson A. 2017. Dok-1 and Dok-2 are required to maintain herpes simplex virus 1-specific CD8+ T cells in a murine model of ocular infection. J Virol 91:e02297-16. https://doi.org/10.1128/JVI.02297-16.

**Editor** Jae U. Jung, University of Southern California



Address correspondence to Pascale Duplay, pascale.duplay@iaf.inrs.ca, or Angela Pearson, angela.pearson@iaf.inrs.ca.

* Present address: Mitra Yousefi, McGill University, Department of Microbiology and Immunology, Montreal, Quebec, Canada.

P.D. and A.P. are co-senior authors.

mucosa and on the cornea, among other sites, and is associated with HSV-1 stromal keratitis, which can lead to blindness (2).

Cell-mediated immunity plays a critical role in limiting viral replication and spread in TG and cornea through the action of cells such as macrophages (3–6), NK cells (7), NKT cells (8), neutrophils (9), and γδ T cells (10). In addition, both $CD4^+$ and $CD8^+$ T cell-mediated immune responses are involved in protection against primary HSV-1 infection (11–14). The majority of HSV-1-specific $CD8^+$ T cells in lymphoid organs during acute infection of B6 mice are directed against a single immunodominant glycoprotein B (gB) epitope (15, 16). During acute infection in an ocular model, HSV-1-specific $CD8^+$ T cells infiltrate sites of infection, namely, the cornea and TG, and promote viral clearance (17). A proportion of HSV-1-specific $CD8^+$ T cells reside in the TG for the life of the animal and are necessary for the maintenance of HSV-1 latency. TG-resident HSV-1-specific $CD8^+$ T cells display an activated phenotype, form close contacts with infected neurons (18–20), remain functional (21), and are tissue-resident memory-type cells (22, 23). In *ex vivo* viral-reactivation assays, depletion of $CD8^+$ T cells from TG cultures increases reactivation frequency, and $CD8^+$ T cells inhibit reactivation of HSV-1 from latency (24, 25).

Dok-1 and Dok-2, two members of the Dok protein family, are preferentially expressed in hematopoietic cells and are involved in the negative regulation of signaling downstream of a variety of immunoreceptors, such as B cell receptor (BCR), T cell receptor (TCR), Fc receptor (FcR), and Toll-like receptor (TLR) (reviewed in references 26, 27, and 28). T cells and myeloid cells express Dok-1 and Dok-2, while B cells express only Dok-1 (28). These two closely related Dok family members are involved in the regulation of several cellular processes, such as proliferation, differentiation, and migration. Using Dok-1- and -2 (Dok-1/2)-deficient mice, biological roles for Dok-1 and Dok-2 have been demonstrated in antibody responses to thymus-dependent antigens, NK and hematopoietic cell development and function, innate immune response to lipopolysaccharide (LPS), myeloid homeostasis, and leukemia suppression (29–36). In addition, we recently demonstrated that Dok proteins regulate the $CD8^+$ T cell response to an exogenous epitope expressed by vaccinia virus (VV) (37). In particular, we showed that Dok proteins negatively regulate the effector function of $CD8^+$ effector T cells and play a critical role in the generation of $CD8^+$ memory T cells (37). As mentioned above, during HSV-1 infection, $CD8^+$ T cells are important in controlling the infection, in particular in maintaining HSV-1 latency (24, 25). In this study, we investigated the impact of Dok-1 and Dok-2 proteins in a model of HSV-1 ocular infection by comparing viral clearance, periocular virus-induced disease, and the HSV-1 gB-specific $CD8^+$ T cell response in wild-type (WT) and Dok-1- and Dok-2-deficient mice. Our data demonstrate that Dok proteins positively control the amplitude of the gB-specific $CD8^+$ T cell response during both the acute and latent phases of HSV-1 infection and are particularly important for the survival of effector memory T (Tem) cells.

## RESULTS

**Dok proteins are not necessary for the control of HSV-1 replication in the cornea and TG during acute infection.** We tested the functional importance of Dok-1 and Dok-2 for viral replication during acute HSV-1 infection using a murine model of ocular infection. Dok-1 and Dok-2 double-knockout (DKO) mice and WT control C57BL/6 mice (referred to here as WT mice) were infected with HSV-1 strain 17, and viral titers in the eye and TG were measured. We observed similar titers in the tear films of DKO and WT mice at 1, 2, and 3 days postinfection (dpi) (Fig. 1A). Similar results were obtained on a different genetic background than C57BL/6 mice, comparing 129/Sv WT and 129/Sv DKO mice (data not shown). At 3 dpi, viral titers in TG for DKO compared to WT mice were of the same magnitude, although we noted a modest reduction (approximately 3-fold lower) for the DKO samples (Fig. 1B). Furthermore, the kinetics of viral clearance in the eyes, monitored from 2 to 8 dpi, were similar for WT and DKO mice (data not shown). Thus, our results show that Dok-1 and Dok-2 are not essential for the control of HSV-1 replication during acute infection.

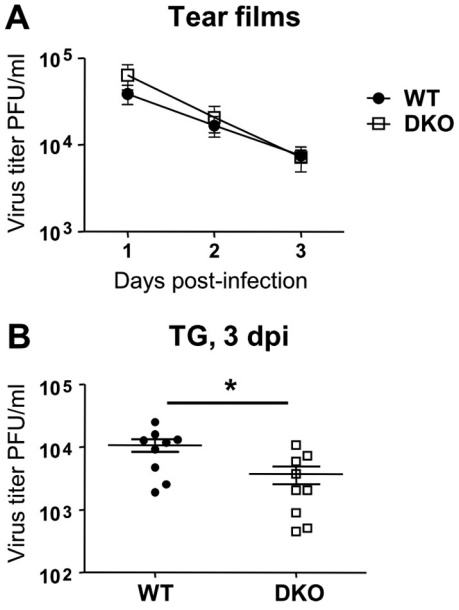


**FIG 1** Impact of Dok proteins on the control of acute HSV-1 replication in the cornea and TG. Shown is quantification of virus titers during acute HSV-1 infection in DKO mice and WT mice. (A) Titers of virus present in tear films of mice 1 to 3 dpi. The data shown were pooled from three independent experiments ($n = 11$ mice). (B) Titers of virus present in the TG at 3 dpi. The data are from four independent experiments. Each symbol represents an individual mouse. Statistical analysis was carried out using a Mann-Whitney test (*, $P < 0.05$). The results are shown as means ± SEM.

**HSV-1-induced clinical signs are not mediated by Dok proteins.** To assess the involvement of Dok-1 and Dok-2 in HSV-induced pathology, we scored in a blinded manner for the severity of disease by daily visual inspection from 4 dpi, when clinical signs begin to appear, to 18 dpi. Following HSV-1 infection, DKO mice developed progressive clinical disease that was similar in kinetics to that observed in WT mice (Fig. 2). Although clinical signs were evident in DKO infected mice, we noted a slight reduction in severity compared to WT mice. There were statistically significant reductions of scores for the DKO mice compared to WT mice at 6 and 7 dpi, although the differences were very small (2.0 versus 2.5 at 6 dpi and 2.1 versus 2.7 at 7 dpi), and inflammatory responses resolved by day 16 in both WT and DKO animals. The influx of innate and adaptive immune cells in the cornea influences early control of the infection and virus-induced inflammation (38, 39). The total numbers of leukocytes (CD45$^+$ cells) infiltrating the corneas and TG of DKO and WT mice at 3 and 8 dpi were similar (Fig. 3B and C). Furthermore, after normalizing each cellular subpopulation to the percentage

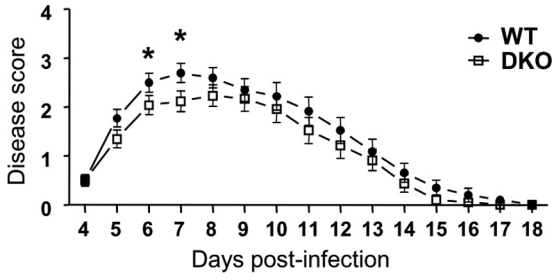


**FIG 2** The absence of Dok proteins does not alter overall periocular HSV-induced inflammation. Following infection of WT and DKO mice, the mean disease score, as determined on a scale of 0 to 4, was assessed each day from 4 to 18 dpi. The graph shows the average scores from data pooled over four independent experiments ($n = 26$). The value indicated for each day is the mean of the values obtained for each animal analyzed on that day postinfection. Statistical analysis was carried out to compare values two by two for WT versus DKO mice at each day using a Mann-Whitney test (*, $P < 0.05$). The results are shown as means ± SEM.

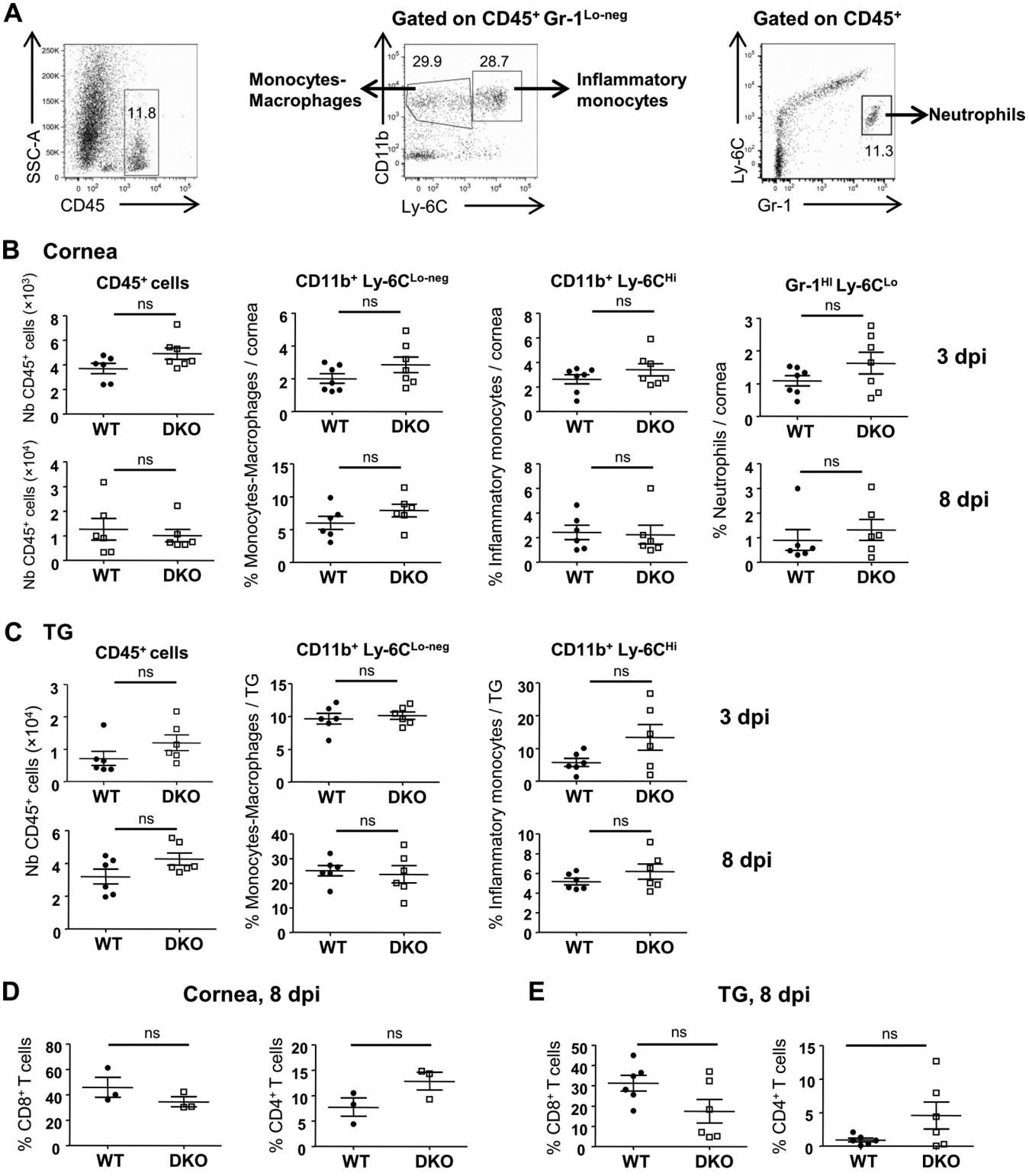


**FIG 3** Dok proteins do not regulate the influx of leukocytes into the cornea and TG during acute infection. (A) Representative gating strategies for leukocyte characterization in the cornea and TG. Live cells from WT cornea at 3 dpi were gated for expression of CD45$^+$ to identify total leukocytes; CD45$^+$ Gr-1$^{Lo\text{-}neg}$ cells were gated for coexpression of CD11b$^+$ Ly-6C$^{Lo\text{-}neg}$ and CD11b$^+$ Ly-6C$^{Hi}$ to identify monocytes/macrophages and inflammatory monocytes, respectively; and CD45$^+$ cells were gated for coexpression of Gr-1$^{Hi}$ and Ly-6C$^{Lo}$ to identify neutrophils. (B) Total numbers (Nb) of leukocytes (CD45$^+$) and the percentages of monocytes/macrophages (CD11b$^+$ Ly-6C$^{Lo\text{-}neg}$), inflammatory monocytes (CD11b$^+$ Ly-6C$^{Hi}$), and neutrophils (Gr-1$^{Hi}$ and Ly-6C$^{Lo}$) among CD45$^+$ cells in corneas at 3 and 8 dpi. (C) Total numbers of leukocytes (CD45$^+$) and percentages of monocytes/macrophages (CD11b$^+$ Ly-6C$^{Lo\text{-}neg}$) and inflammatory monocytes (CD11b$^+$ Ly-6C$^{Hi}$) among CD45$^+$ cells in TG at 3 and 8 dpi. (B and C) Each symbol represents one mouse, where the two eyeballs (B) or two TG (C) were pooled prior to analysis. (D and E) Percentages of total CD8$^+$ and CD4$^+$ T cells among CD45$^+$ cells in the cornea (D) and TG (E) at 8 dpi. The data shown represent the pooled results from three independent experiments, and each symbol represents two mice (D) or one mouse (E). Statistical analysis was carried out using a Mann-Whitney test. ns, not significant. The results are shown as means ± SEM.

of CD45$^+$ cells, we found similar percentages of inflammatory monocytes and monocytes/macrophages infiltrating in corneas and TG for DKO and WT mice at 3 and 8 dpi (Fig. 3A to C). The percentages of neutrophils were also similar in corneas of DKO and WT mice at 3 and 8 dpi (Fig. 3B). In addition, the numbers of CD4$^+$ and CD8$^+$ T cells in corneas and TG of DKO and WT mice at 8 dpi were similar (Fig. 3D and E). Together, these results suggest that early during infection, the absence of Dok proteins does not have a major impact on the overall periocular HSV-induced inflammation or on leukocyte influx in the cornea.

**Dok proteins positively regulate the HSV-1-specific CD8$^+$ T cell response in the spleen and draining lymph nodes.** We tested the importance of Dok proteins in the expansion of HSV-1-specific CD8$^+$ T cells. At 8 dpi, which corresponds to the peak of the response in WT B6 mice (40), the number of HSV-1-specific CD8$^+$ T cells was assessed using H2K$^b$ gB tetramers corresponding to the immunodominant HSV-1 epitope (15). DKO mice exhibited a significant decrease in the absolute numbers and percentages of gB-specific CD8$^+$ T cells in the spleen (4-fold lower in absolute numbers) and draining lymph nodes (dLN) (approximately 2-fold lower in absolute numbers) compared to WT mice (Fig. 4A to C). This decrease was not due to a reduction of total CD8$^+$ T cells in the spleen or dLN because the absolute CD8$^+$ T cell numbers were similar in DKO and WT mice (data not shown). WT and Dok-1 or Dok-2 single-KO mice exhibited similar absolute numbers of gB-specific CD8$^+$ T cells in the spleen at 8 dpi (data not shown). These results are consistent with previous studies that showed redundant functions for Dok-1 and Dok-2 (34). We next assessed the gB-specific CD8$^+$ T cell response in the spleen at a time corresponding to a latent infection. At 43 dpi, the absolute number and percentage of gB-specific CD8$^+$ T cells in the spleen were significantly reduced in DKO mice compared to WT mice (Fig. 4D). Moreover, the number of gB-specific CD8$^+$ T cells in DKO mice was below the level of detection, producing values similar to those corresponding to background nonspecific tetramer staining. Thus, our data demonstrate that Dok-1 and Dok-2 proteins are critical for the maintenance of gB-specific memory CD8$^+$ T cells in the spleen.

**Dok proteins do not regulate the proportion of effectors and memory CD8$^+$ T cell precursors or the functional abilities of gB-specific CD8$^+$ T cells at the effector phase.** We examined if the disappearance of gB-specific CD8$^+$ T cells in DKO mice was due to an inability of gB-specific CD8$^+$ T cells to differentiate into memory precursor effector cells (MPECs). To address this question, we assessed the proportions of short-lived effector cells (SLECs) and MPECs by evaluating expression of KLRG1 and CD127 on gB-specific CD8$^+$ T cells in the spleen at 8 dpi. The proportion of SLECs (KLRG1$^{Hi}$ CD127$^{Lo}$) and the proportion of MPECs (KLRG1$^{Lo}$ CD127$^{Hi}$) were similar in DKO and WT mice (Fig. 5A), suggesting that Dok-1 and Dok-2 do not modulate the proportions of effector and memory CD8$^+$ T cell precursors.

To determine if the functional capacity of splenocytes from infected DKO mice was altered, we examined gamma interferon (IFN-$\gamma$), tumor necrosis factor alpha (TNF-$\alpha$), and granzyme B (GrzB) synthesis in response to stimulation *ex vivo* with a peptide corresponding to the HSV-1 gB epitope in the presence of anti-CD107a monoclonal antibody (MAb) (to detect lytic-granule release). Since there were fewer gB-specific CD8$^+$ T cells in DKO mice, we normalized the IFN-$\gamma$/TNF-$\alpha$ secretion (IFN-$\gamma^{Hi}$ TNF-$\alpha^{Hi}$ cells) or cytotoxic response (GrzB$^{Hi}$ CD107a$^{Hi}$) to the numbers of tetramer$^+$ (Tet$^+$) CD8$^+$ cells present in the spleens of DKO and WT mice. While we observed a small decrease in the relative numbers of IFN-$\gamma^{Hi}$ TNF-$\alpha^{Hi}$ cells and in the relative cytotoxic response of gB-specific CD8$^+$ T cells in DKO mice compared to those in WT mice, the differences were not significant (Fig. 5B and C). Although our evidence suggests that the Dok-1 and Dok-2 proteins do not modulate the functional abilities of gB-specific CD8$^+$ T cells, given the trend we observed, we cannot completely rule out this possibility.

**Dok proteins regulate the number of gB-specific CD8$^+$ Tem cells in the spleen.** It was possible that HSV-1 infection resulted in the generation of CD8$^+$ T cells with different abilities to survive and to respond to antigen after the effector phase. To address this possibility, we compared the memory phenotype (CD44$^{high}$ CD62L$^-$

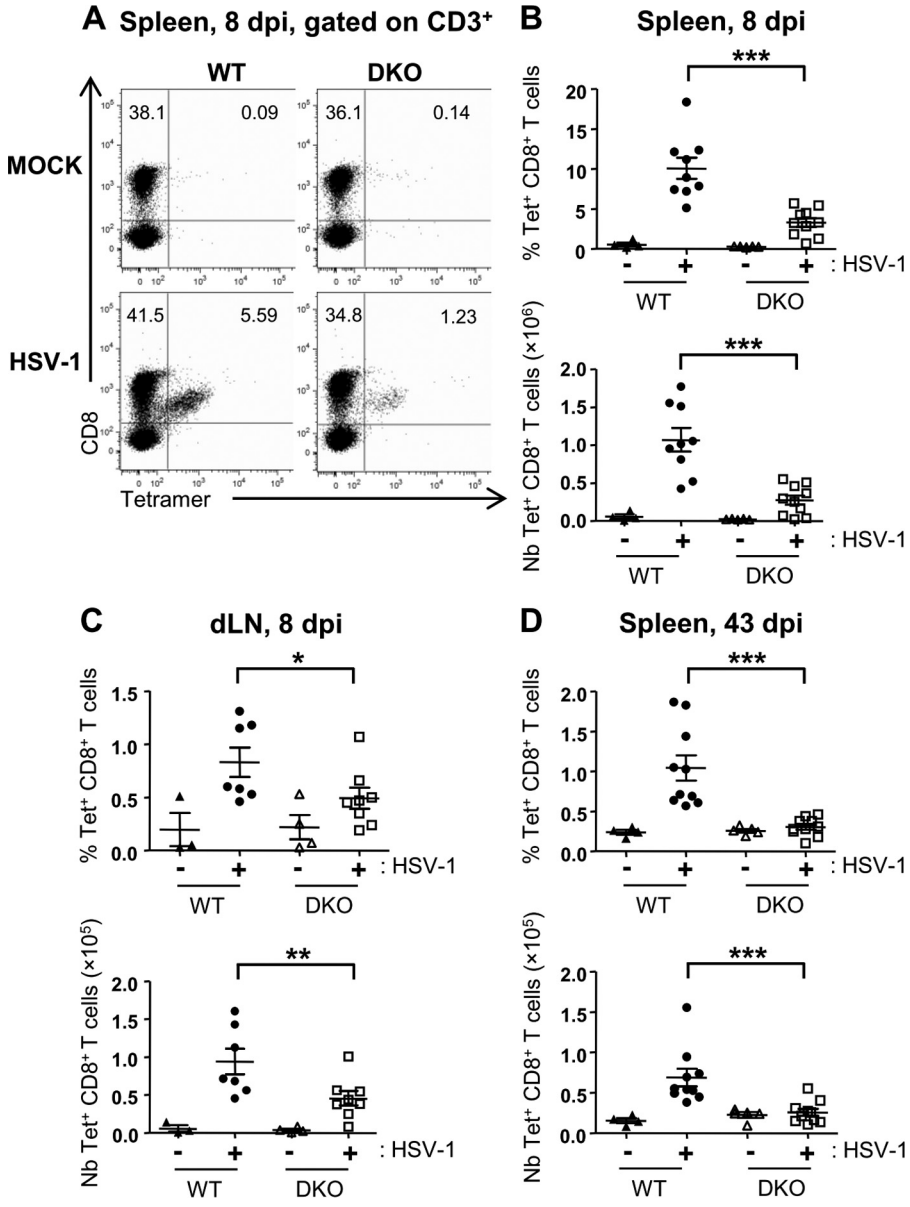


**FIG 4** Dok proteins positively regulate the number of gB-specific CD8$^+$ T cells in the spleen and dLN. WT and DKO mice were infected with HSV-1 or not (Mock), and then spleens or dLN were harvested at the indicated times and stained with anti-CD3, anti-CD8, and H2-K$^b$ gB tetramers. (A) Representative dot plots of gB-specific CD8$^+$ T cells gated on CD3$^+$ cells. (B to D) Frequencies of gB-specific CD8$^+$ T cells (%Tet$^+$ CD8$^+$ T cells) (top) and absolute numbers of gB-specific CD8$^+$ T cells (Nb Tet$^+$ CD8$^+$ T cells) (bottom) in the spleen (B) and dLN (C) at 8 dpi and in the spleen at 43 dpi (D). The data shown represent the pooled results from four (B) or three (C and D) independent experiments. Each symbol represents an individual mouse. Statistical analysis was carried out to compare values two by two for WT versus DKO mice using a Mann-Whitney test (***, $P < 0.001$; **, $P < 0.01$; *, $P < 0.05$). The results are shown as means ± SEM.

Tem/CD44$^{high}$ CD62L$^+$ central memory T [Tcm] cells) and the rates of proliferation of gB-specific CD8$^+$ T cells in the spleens of HSV-1-infected WT and DKO mice at an early phase (14 dpi) and at a later phase (33 dpi) of effector-to-memory CD8$^+$ T cell transition. At 14 dpi and 33 dpi, DKO mice had significantly lower percentages of gB-specific CD8$^+$ Tem cells in spleen (Fig. 6A and B) and blood (data not shown) than their WT counterparts. By 33 dpi, there were 6-fold fewer gB-specific CD8$^+$ Tem cells and 2-fold fewer gB-specific CD8$^+$ Tcm cells in the spleens of DKO mice than in those of WT mice (Fig. 6B). Of note, no such reduction in the number of CD8$^+$ Tem cells was observed in the total CD44$^+$ memory CD8$^+$ T cell population between WT and DKO mice at 33 dpi (Fig. 6C).

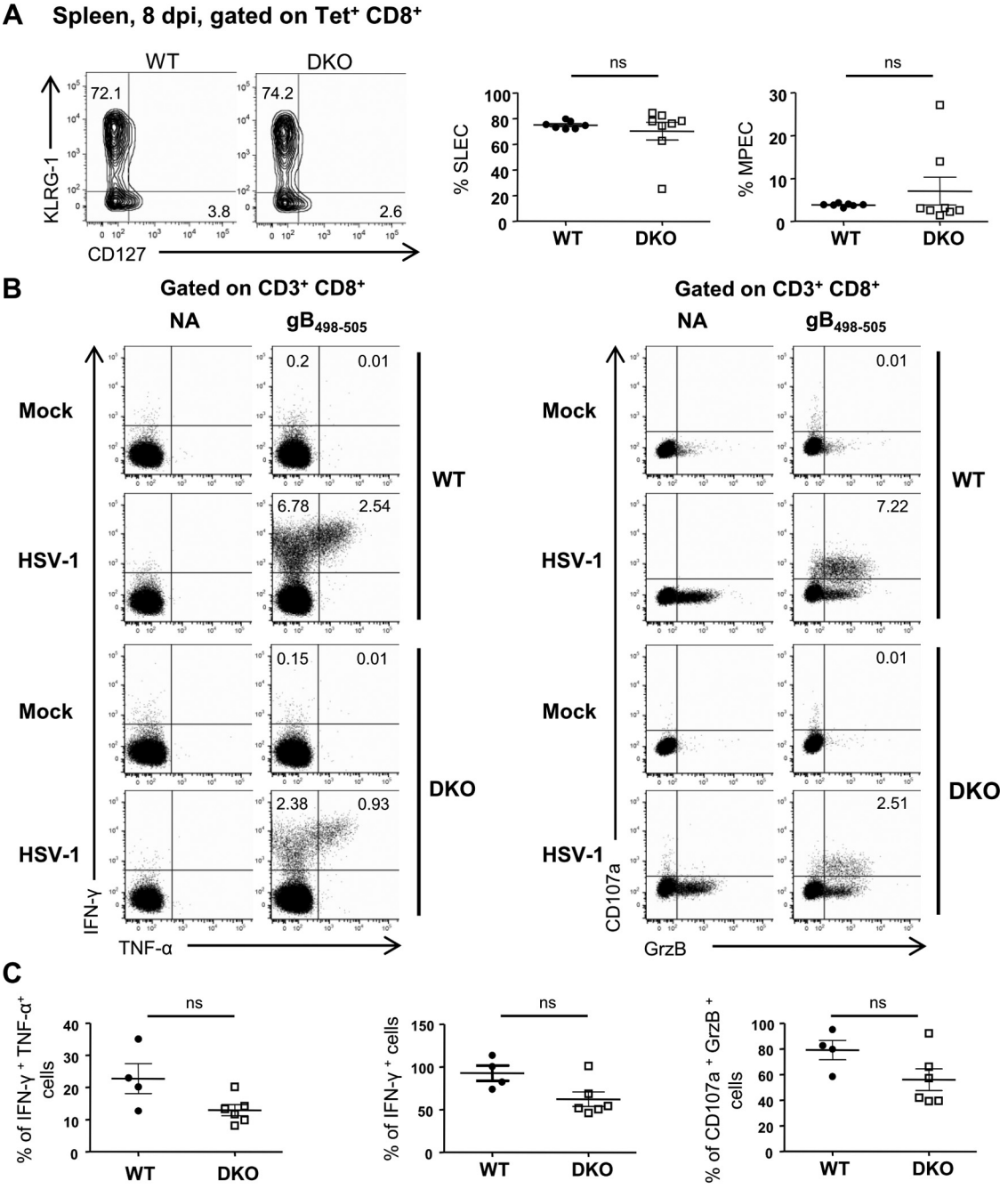


**FIG 5** Dok proteins do not modulate the proportions of effectors and memory CD8$^+$ T cell precursors or the functional abilities of gB-specific CD8$^+$ T cells. (A) (Left) Representative dot plot gated on gB-specific CD8$^+$ T cells (Tet$^+$ CD8$^+$) showing KLRG-1 and CD127 in the spleen at 8 dpi. (Right) Percentages of SLECs (KLRG1$^{Hi}$ CD127$^{Lo}$) and MPECs (KLRG1$^{Lo}$ CD127$^{Hi}$). The data represent the pooled results from three independent experiments. Each symbol represents an individual mouse. (B and C) WT and DKO mice were infected with HSV-1 or not (Mock), and splenocytes harvested at 8 dpi were stimulated *ex vivo* with gB peptide or left in medium (nonactivated [NA]) for 4 h. (B) Plots gated on CD3$^+$ CD8$^+$ cells showing IFN-$\gamma$ and TNF-$\alpha$ expression and CD107a and GrzB expression. (C) Representative graphs showing the percentages of IFN-$\gamma^+$ TNF-$\alpha^+$, IFN-$\gamma^+$, and CD107a$^+$ GrzB$^+$ cells among Tet$^+$ CD8$^+$ cells. The numbers were obtained by dividing the percentage of cytokine$^+$ cells in the CD8$^+$ CD3$^+$ cell population by the percentage of gB-tetramer$^+$ cells before *ex vivo* stimulation of the cells. The data shown represent results pooled from two independent experiments. Each symbol represents an individual mouse. Statistical analysis was carried out using a Mann-Whitney test. ns, not significant. The results are shown as means ± SEM.

We also assessed the proportion of actively cycling cells *in vivo* by giving mice an injection of bromodeoxyuridine (BrdU) 12 h before harvesting the cells. Staining cells for BrdU incorporation at 8, 14, and 33 dpi showed that the percentages of cycling BrdU$^+$ WT and DKO gB-specific CD8$^+$ cells were very similar (Fig. 6D). This result

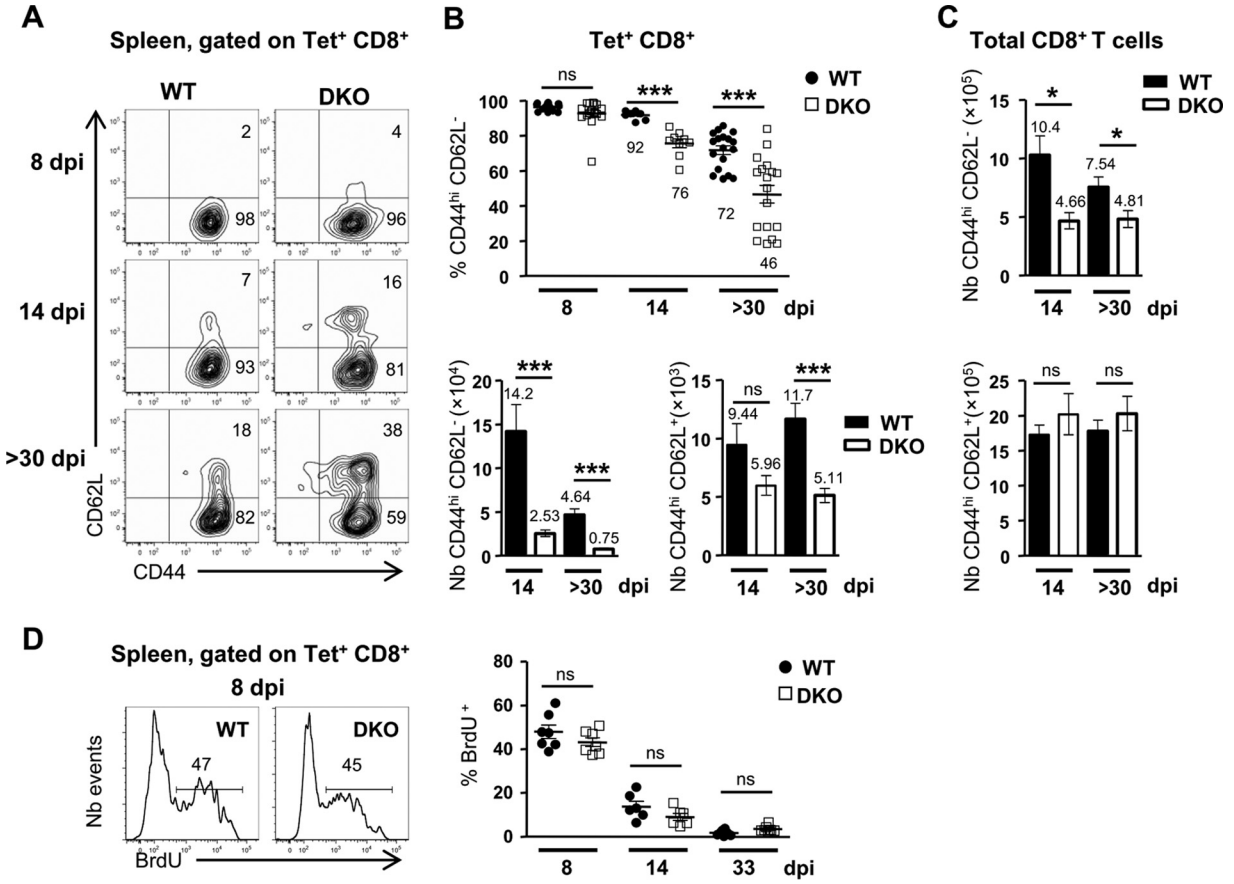


**FIG 6** Reduced numbers of gB-specific CD8$^+$ Tem cells are present in the spleens of Dok-1/2 DKO mice. (A) Representative contour plot gated on gB-specific CD8$^+$ T cells (Tet$^+$ CD8$^+$) showing CD44 and CD62L in the spleen at 8, 14, and >30 (33 to 48) dpi. (B) (Top) Percentages of gB-specific CD8$^+$ T cells (CD44$^{Hi}$ CD62L$^-$) in the spleen at 8, 14, and >30 (33 to 48) dpi. Each symbol represents an individual mouse. The numbers below the symbols indicate the means. (Bottom) Absolute numbers of gB-specific CD8$^+$ T cells (CD44$^{Hi}$ CD62L$^-$) and gB-specific CD8$^+$ T cells (CD44$^{Hi}$ CD62L$^+$) in the spleen at 8, 14, and >30 dpi. The error bars indicate the standard deviations, and the numbers above indicate the means. The results are representative of five independent experiments (8 dpi), four independent experiments (>30 dpi), and two independent experiments (14 dpi), with at least two mice analyzed per condition in each experiment. (C) Absolute numbers of total CD8$^+$ T cells (CD44$^{Hi}$ CD62L$^-$ [top] and CD44$^{Hi}$ CD62L$^+$ [bottom]) in the spleen at 8, 14, and >30 (33 to 48) dpi. The error bars indicate standard deviations, and the numbers above indicate the means. (D) Mice were given an intraperitoneal injection of BrdU, and spleens were harvested 12 h after BrdU exposure. Cells were stained with anti-CD3, anti-CD8, and H2-K$^b$ gB tetramers and then for BrdU incorporation at the indicated times. (Left) Representative histograms gated on gB-specific CD8$^+$ T cells (Tet$^+$ CD8$^+$) showing the percentages of BrdU$^+$ cells. (Right) Kinetics of percentages of gB-specific CD8$^+$ BrdU$^+$ T cells. The data shown are from six to eight mice per condition tested. Each symbol represents an individual mouse. Statistical analysis was carried out using a Mann-Whitney test (***, $P < 0.001$; *, $P < 0.05$; ns, not significant).

indicates that the reduced numbers of gB-specific CD8$^+$ T cells in the DKO spleen is due their reduced survival rather than an impaired proliferative capacity.

**Dok proteins positively regulate the numbers of HSV-1-specific CD8$^+$ T cells recruited to the cornea and TG.** We showed that Dok-1 and Dok-2 proteins are required for maintenance of the gB-specific CD8$^+$ T cell response in lymphoid tissues. To determine whether the same effect occurs in nonlymphoid tissues, we extended our analyses to TG and cornea during acute and latent infection. To ensure sufficient numbers of cells for accurate counts, two to four TG were pooled for each data point, and four eyeballs were pooled for each sample tested. We quantified gB-specific CD8$^+$ T cells among CD45$^+$ CD3$^+$ cells. Although the total numbers of CD8$^+$ T cells infiltrating TG were reproducibly reduced in DKO mice in comparison to WT mice at 8, 14, and >30 dpi, the numbers did not reach statistical significance (Fig. 7A). Importantly, at 8 and 14 dpi, the percentage of gB-specific CD8$^+$ T cells among total CD8$^+$ T cells and the number of gB-specific CD8$^+$ T cells were significantly reduced in TG from DKO mice compared to those from WT mice (approximately 1.5-fold lower and 2-fold lower, respectively) (Fig. 7B and C). During latency (>30 dpi), the reduction of gB-specific

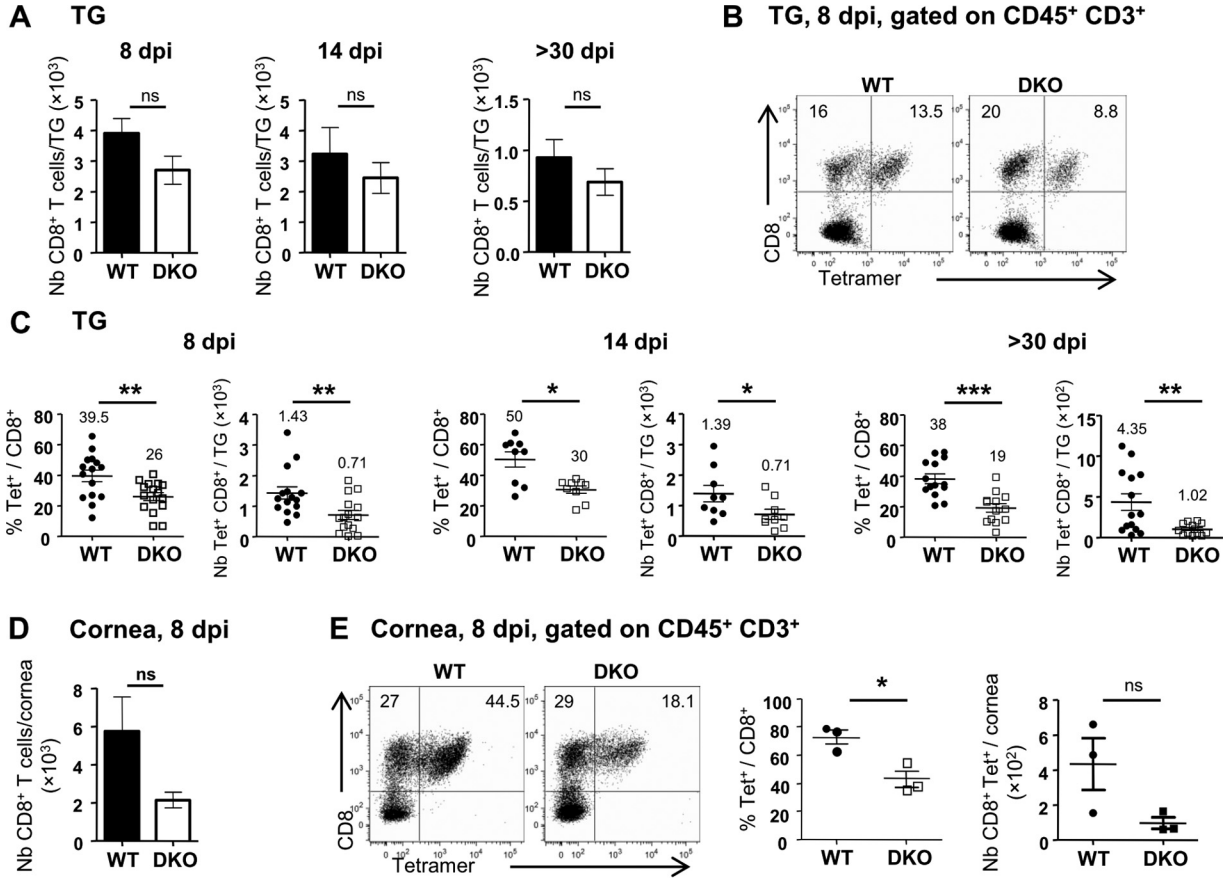


**FIG 7** Dok proteins positively regulate gB-specific CD8+ T cells recruited to the cornea and TG. (A to C) WT and DKO mice were infected with HSV-1, and TG were harvested at 8, 14, and >30 (33 to 48) dpi. The graphs show the total numbers of CD8+ T cells per TG (A) and the percentages and numbers of gB-specific CD8+ T cells per TG (C). (B) Representative dot plots of CD45+ CD3+ cells stained with anti-CD8 MAbs and gB tetramers at 8 dpi. The data shown are pooled from five independent experiments (8 dpi), four independent experiments (>30 dpi), and two independent experiments (14 dpi). Each individual symbol corresponds to one or two mice (two or four TG). (D and E) Corneas were harvested at 8 dpi. (D) Numbers of CD8+ T cells per cornea. (E) Representative dot plots of CD45+ CD3+ cells stained with anti-CD8 MAbs and gB tetramers (left) and graphs illustrating the percentages and numbers of gB-specific CD8+ T cells per cornea (right). The data shown are pooled from three independent experiments, and each symbol represents two mice (four corneas). Statistical analysis was carried out using a Mann-Whitney test (***, $P < 0.001$; **, $P < 0.01$; *, $P < 0.05$; ns, not significant). The results are shown as means ± SEM.

CD8+ T cells in DKO TG was even more pronounced (approximately 4-fold lower) (Fig. 7C). In the cornea at 8 dpi, DKO mice also exhibited a significant decrease in the percentage of gB-specific CD8+ T cells among total CD8+ T cells (approximately 2-fold lower). Although not significant, there was a reduction in the numbers of total and of gB-specific CD8+ T cells (3-fold and 4.5-fold lower) (Fig. 7D and E) compared to WT mice. Just as was seen in the spleen, the proliferation of gB-specific CD8+ T cells in the TG in WT mice was similar to that in DKO mice (Fig. 8A). The PD-1–B7-H1 interaction has been shown to be important for the survival of CD8+ resident T cells in TG (41). Expression of PD-1 is also associated with reduced functionality (41, 42). We next determined whether there was a difference in the expression of PD-1 receptor. At 8, 14, and 33 dpi, PD-1 expression levels on WT and DKO gB-specific CD8+ T cells in TG were similar (Fig. 8B). In addition, the majority of gB-specific CD8+ T cells displayed similar CD44$^{high}$ CD62L− Tem phenotypes in WT and Dok-1/2 DKO TG (Fig. 8C). Likewise, at 33 dpi, the percentages of CD103+ gB-Tet+ and gB-Tet− CD8+ memory resident T cells were similar in WT and DKO TG (Fig. 8D). In conclusion, in acutely (8 dpi) and latently (>30 dpi) infected TG, WT and DKO gB-specific CD8+ T cells were phenotypically similar. Moreover, the fold difference found in the frequencies and numbers of gB-specific CD8+ T cells between WT and DKO mice progressively increased during the contraction phase of the effector cells in the TG. These results suggest that reduced

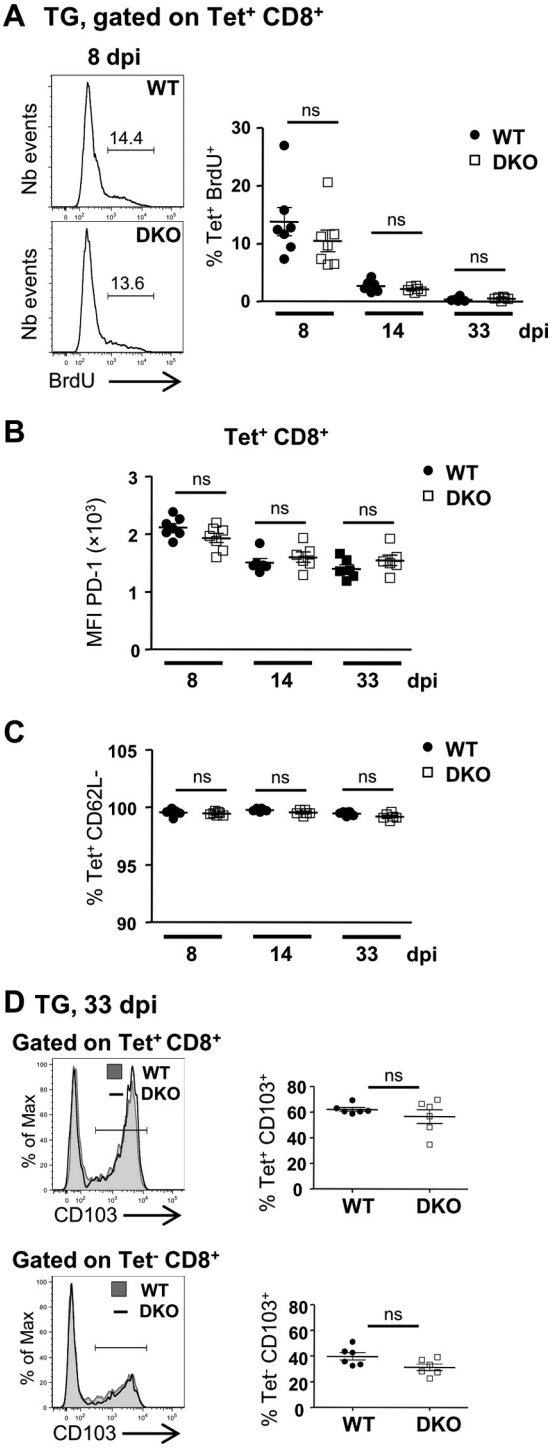


**FIG 8** Dok-1/2 DKO CD8$^+$ T cells in TG are phenotypically similar to WT cells. (A) Mice were given an intraperitoneal injection of BrdU, and TG were harvested 12 h after BrdU exposure. Cells were stained with anti-CD3, anti-CD8, and H2-K$^b$ gB tetramers and then for BrdU incorporation at the indicated times. (Left) Representative histograms gated on gB-specific CD8$^+$ T cells (Tet$^+$ CD8$^+$) showing the percentages of BrdU$^+$ cells. (Right) Kinetics of percentages of gB-specific CD8$^+$ BrdU$^+$ T cells. (B and C) Mean fluorescence intensities (MFI) of PD1 expression on gB-specific CD8$^+$ T cells (B) and percentages of CD62L$^-$ gB-specific CD8$^+$ T cells (C). (D) (Left) Representative histograms gated on gB-specific CD8$^+$ T cells (Tet$^+$ CD8$^+$) and gB tetramer$^-$ cells (Tet$^-$ CD8$^+$) showing the percentages of CD103$^+$ cells at 33 dpi. (Right) Percentages of CD103$^+$ cells gated on gB tetramer$^+$ (Tet$^+$) and gB tetramer$^-$ (Tet$^-$) CD8$^+$ T cells. The data shown are from six to eight mice per condition tested. Each symbol represents an individual mouse. Statistical analysis was carried out using a Mann-Whitney test. ns, not significant. The results are shown as means ± SEM.

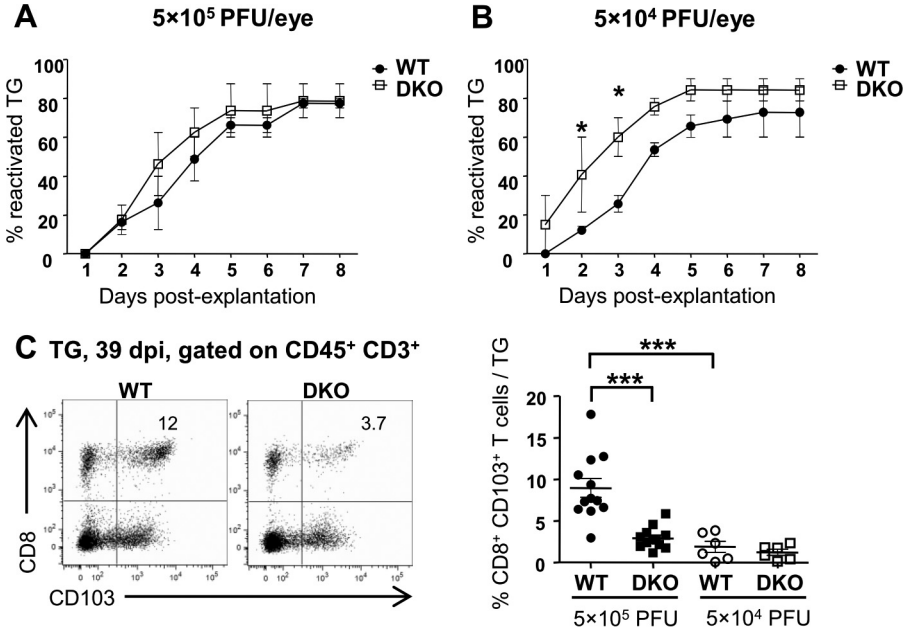


**FIG 9** Dok proteins hinder HSV-1 reactivation from latency in *ex vivo* cultures of TG. (A and B) WT and DKO mice were infected with $5 \times 10^5$ PFU/eye (A) or $5 \times 10^4$ PFU/eye (B) of HSV-1, and TG were harvested following the establishment of latency and dissociated. Half of each TG sample was tested in an *ex vivo* reactivation assay by daily monitoring for virus-induced cytopathic effects of Vero cells on which the dissociated TG was overlaid. The graphs show the percentages of reactivated TG on the indicated days postexplant. The data shown were pooled from two independent experiments ($n = 24$ [A] and $n = 18$ [B]). Statistical analysis was carried out using a chi-squared test (*, $P < 0.05$). (C) The other half of each TG tested in an *ex vivo* reactivation assay was pooled and analyzed by cytometry to quantify TG-resident CD8+ T cells. (Left) Representative dot plot of TG-resident CD8+ T cells (CD8+ CD103+) gated on CD45+ CD3+ cells in TG at 36 to 39 dpi. (Right) Percentages of TG-resident CD8+ T cells per TG at high ($5 \times 10^5$ PFU/eye) and low ($5 \times 10^4$ PFU/eye) infectious doses. The data represent the results from three ($5 \times 10^5$ PFU/eye) or two ($5 \times 10^4$ PFU/eye) independent experiments. Statistical analysis was carried out to compare values two by two for WT versus DKO mice and for WT mice at two infectious doses using a Mann-Whitney test (*, $P < 0.05$; ***, $P < 0.001$). The results are shown as means ± SEM.

numbers of gB-specific CD8+ T cells infiltrate the acutely infected TG (8 dpi) in DKO mice and that the survival of DKO gB-specific CD8+ T cells in the TG is reduced compared to WT cells.

**Absence of Dok proteins promotes HSV-1 reactivation from latency in *ex vivo* TG cultures.** CD8+ T cells specific for the immunodominant gB epitope are functional in latently infected TG and contribute to the control of HSV-1 reactivation from latency (21, 24). Furthermore, the frequency of HSV-1 reactivation from latency in *ex vivo* TG cultures has been shown to correlate inversely with the number of infiltrating CD8+ T cells (25). Since the lack of Dok-1 and Dok-2 proteins caused a decrease in the proportion and numbers of gB-specific CD8+ T cells present in TG during HSV-1 latency, we tested the impact of Dok proteins on HSV-1 reactivation from latency in *ex vivo* TG cultures. At an infectious dose of $5 \times 10^5$ PFU/eye, despite the fact that viral DNA was more readily detected in TG from latently infected WT mice than in TG from DKO mice (12/13 versus 8/13 HSV-1-positive samples, respectively), reactivation was detected on average a half day earlier from infected DKO TG than from WT TG (3.6 versus 4.1 days postexplant) (Fig. 9A). This trend became significant at a lower infectious dose ($5 \times 10^4$ PFU/eye), where reactivation was detected on average 1.1 days ($P \leq 0.05$) earlier for the DKO TG than for WT TG. Moreover, the percentage of reactivated TG from DKO mice was significantly greater at 2 and 3 days postexplant than for WT mice (Fig. 9B). As shown in Fig. 9C, at a high infectious dose, there was a high percentage of CD103+ CD8+ T cells in TG of WT mice, while the percentage was significantly lower in TG of DKO mice (8.9% for WT and 2.9% for DKO mice). Consistent with previous reports, at a low infectious dose, the percentage of memory-resident CD103+ CD8+ T cells was

reduced compared to that observed for a high infectious dose (25); however, at the lower infectious dose, the percentage of TG-resident CD8$^+$ T cells was too close to the background nonspecific staining for DKO mice to accurately assess the difference between WT and DKO samples. Our results suggest that Dok proteins have a negative impact on HSV-1 *ex vivo* reactivation from latency.

## DISCUSSION

In this study, we examined the roles of Dok-1 and Dok-2 in regulating HSV-1 infection in a mouse model of ocular infection. We found that Dok-1 and Dok-2 are important for the formation of long-lived HSV-1-specific CD8$^+$ T cells in lymphoid and nonlymphoid organs. We previously reported the importance of Dok-1/2 in memory T cell formation in response to vaccinia virus expressing OVA peptide using an adoptive-transfer system of DKO OT-I cells (37). Just as we showed for VV OVA infection, the number of HSV-specific CD8$^+$ T cells in response to HSV-1 infection was diminished at the peak of the effector response. Thus, the fate of HSV-specific DKO CD8$^+$ T cells in the present study was similar to that obtained with OVA-specific DKO CD8$^+$ OT-I T cells adoptively transferred into WT mice in our previous study. Although we cannot exclude other hypotheses, this finding suggests that the defect in the formation of gB-specific CD8$^+$ memory T cells in DKO mice is T cell intrinsic. Moreover, we demonstrated that Dok proteins are dispensable for differentiation of MPECs, suggesting that Dok proteins do not regulate the differentiation of gB-specific CD8$^+$ memory precursor T cells. Nevertheless, our data clearly indicate that the survival of CD8$^+$ Tem cells is more affected than that of CD8$^+$ Tcm cells. Because of the importance of CD8$^+$ Tem cells in protective immunity against herpesvirus infection (43, 44), studies aimed at gaining a better understanding of how Dok-1/2 deficiency affects the survival of gB-specific CD8$^+$ Tem cells are under way.

In addition to T and B cells, Dok-1 and Dok-2 proteins are expressed in myeloid cells (28). We have previously shown that in IFN-$\gamma$-primed macrophages, nitric oxide (NO) and TNF secretion is reduced in DKO cells (45). Thus, Dok-1/2 deficiency could be expected to result in less efficient clearing of the virus during acute infection; however, we found that viral titers in tear films and the kinetics of viral clearance in the eyes were similar in DKO and WT mice. This observation was consistent with our finding that there were no statistically significant differences in the degrees of leukocytic infiltration (monocytes/macrophages, neutrophils, inflammatory monocytes, and T cells) into the cornea at 3 and 8 dpi in DKO and WT mice. In contrast, we showed that the numbers of gB-specific CD8$^+$ T cells were reduced in the cornea but that Dok-1 and Dok-2 deficiency did not affect *ex vivo* functional abilities. Thus, our results imply that although the number of gB-specific T cells is lower in DKO mice, there were sufficient cells to clear the virus.

We found that reactivation in *ex vivo* TG cultures was detected earlier for DKO than for WT mice. This observation was surprising, because viral titers in TG were reduced during acute infection of DKO mice versus WT mice. Several studies have suggested that CD8$^+$ T cells resident in the TG delay HSV-1 reactivation from latency (24, 25). Thus, the apparent contradiction of more efficient reactivation despite lower viral titers in TG during acute infection may be due to the reduced numbers of HSV-1-specific resident CD8$^+$ T cells in DKO TG during the latent phase. It should be noted that we assessed only the gB-specific HSV-1 CD8$^+$ T cell response (15); however, the HSV-specific CD8$^+$ TCR repertoire recognizes other subdominant epitopes (46), and it remains to be determined if Dok proteins affect the entire HSV-specific CD8$^+$ T cell repertoire. Regardless, subdominant CD8$^+$ T cells should not be capable of blocking reactivation, since TG-resident CD8$^+$ T cells specific for subdominant epitopes lose functionality, whereas those specific for the immunodominant gB epitope exhibit increased functionality in latently infected TG (21). In addition, regardless of the HSV specificity of the CD8$^+$ T cells in latently infected TG, we clearly demonstrated that Dok proteins control the number of CD8$^+$ T cells that harbor a resident phenotype as assessed by the CD103$^+$ marker (23). Thus, Dok-1 and Dok-2 may contribute to protection against HSV-1 reactivation from latency by controlling the numbers of HSV-specific CD8$^+$

resident T cells in the TG. Further studies are required to determine whether Dok-mediated regulation of the kinetics of HSV-1 reactivation is mediated exclusively by HSV-specific CD8$^+$ T cells. In particular, we cannot exclude the possibility that Dok proteins regulate the functionality or the numbers of cells other than CD8$^+$ T cells, such as CD8$\alpha^+$ dendritic cells (DCs), that contribute to the establishment and maintenance of HSV latency (47, 48). Future studies will help to delineate the precise functions of Dok proteins in latent HSV-1 infection.

In conclusion, our findings identify Dok-1 and Dok-2 as novel cellular immune regulators in HSV-1 infection that are important for promoting the maintenance of HSV-1 gB-specific CD8$^+$ T cells. As such, Dok proteins promote latency in TG. Elucidation of the mechanisms by which Dok proteins may hinder HSV-1 reactivation from latency could provide insights into possible strategies to block HSV-1 reactivation.

## MATERIALS AND METHODS

**Mice and virus strains.** HSV-1 strain 17 was originally provided by Donald M. Coen (Harvard Medical School). The virus was propagated and titrated on Vero cells as described previously (49). Dok-1-deficient (Dok-1 KO) mice, Dok-2-deficient (Dok-2 KO) mice, and Dok-1/Dok-2 double-deficient (DKO) mice have been described previously (37). All colonies were maintained under pathogen-free conditions at the INRS Centre for Experimental Biology. All animal experiments were performed at the INRS Centre for Experimental Biology in accordance with institutional good animal care practices.

**Flow cytometry reagents.** The gB peptide ($_{498}$SSIEFARL$_{505}$) was purchased from Genemed Synthesis, Inc. H-2K$^b$ tetramers complexed with the gB peptide and coupled to phycoerythrin (PE), allophycocyanin (APC), or brilliant violet 421 were kindly provided by the National Institutes of Health Tetramer Core Facility (Emory University, Atlanta, GA). Fluorescein isothiocyanate (FITC)-conjugated, Alexa Fluor 700-conjugated, or APC-conjugated anti-CD8$\alpha$ (clone 53-6.7); APC-conjugated, APC/Cy7-conjugated, or brilliant violet 421-conjugated anti-CD3$\varepsilon$ (clone 145-2C11); PE/Cy7-conjugated anti-CD4 (clone GK1.5); Alexa Fluor 700-conjugated anti-CD45 (clone 30-F11); FITC-conjugated anti-CD107a (clone 1D4B); PE-conjugated anti-KLRG1 (clone 2F1/KLRG1); FITC-conjugated anti-CD127 (clone A7R34); APC-conjugated anti-IFN-$\gamma$ (clone XMG1.2); brilliant violet 650-conjugated anti-TNF-$\alpha$ (clone MP6-XT22); PE-conjugated anti-CD103 (clone 2E7); APC/Cy7-conjugated anti-Ly-6C (clone HK1.4); APC/Cy7-conjugated or PE-conjugated anti-CD44 (clone IM7); PE-conjugated or PE/Cy7-conjugated anti-CD62L (clone MEL-14); brilliant violet 605-conjugated anti-CD279 (PD-1 clone 29F.1A12); and 7-aminoactinomycin D (7-AAD) viability staining solution were purchased from Biolegend. PE-conjugated anti-GrzB (clone NGZB), APC/Cy7-conjugated anti-Gr-1 (clone RB6-8C5), streptavidin-PE/Cy5, and intracellular fixation and permeabilization buffer (plus brefeldin A) were purchased from eBioscience. FITC-conjugated anti-CD11b (clone M1/70), the FITC BrdU flow kit, and the BD CompBeads Compensation Particles set were obtained from BD Biosciences.

**Murine model of ocular infection.** Six- to 12-week-old male mice were deeply anesthetized by intraperitoneal injection of ketamine (75 mg kg of body weight$^{-1}$; Bioniche) and xylazine (10 mg kg$^{-1}$; Bayer) in saline solution. The corneas of the anesthetized mice were lightly scarified 12 times with a sterile 30-gauge needle, and each eye was infected with 5 $\mu$l of Dulbecco's modified Eagle's medium (DMEM) containing $5 \times 10^5$ PFU of virus unless otherwise indicated. Analyses of acute replication in the eye and TG were conducted essentially as described previously (50). Viral titers were determined for three mice per condition in the eye and for two or three mice per condition in TG. Back titers of inocula were verified following infection of the mice. Data points below the level of detection of the experiment were treated as the limit values for calculation of means.

**Disease scoring.** Acute disease was assessed visually daily in a blind manner for the indicated period and scored on a scale of 0 to 4 as follows: 0, no change; 1, mild inflammation (swelling); 2, moderate inflammation and mild periocular hair loss; 3, severe inflammation, moderate periocular hair loss, and mild skin lesions; and 4, severe inflammation, severe periocular hair loss, and severe skin lesions.

**Flow cytometry and tetramer staining.** At the indicated times postinfection (p.i.), spleens and dLN were removed and dissociated mechanically to obtain single-cell suspensions using 100-$\mu$m nylon cell strainers (BD Falcon). Pooled TG (2 TG equivalents) and pooled eyeballs (4 eyeball equivalents) were incubated in DMEM containing 51 U/ml of collagenase type 1 (Invitrogen) for 1 to 2 h at 37°C, dispersed into single-cell suspension by pipetting, and filtered through 40-$\mu$m-pore-size filters to remove debris prior to staining. Spleens and TG were treated with red blood cell lysis buffer prior to their use, as described previously (37). Single-cell suspensions of various organs were stained with gB tetramers for 30 min at room temperature (RT), followed by cell surface marker staining for 20 min at 4°C in fluoresence-activated cell sorter (FACS) buffer (phosphate-buffered saline [PBS], 1% fetal bovine serum, 0.05% sodium azide, 2 mM EDTA). For TG and corneas, anti-CD45 was added to permit gating exclusively on bone marrow-derived cells. Cells were washed and fixed with 1% paraformaldehyde (PFA) and analyzed by flow cytometry. Dead cells were excluded by selective gating on 7-AAD-negative cells. Data were acquired on a BD LSR Fortessa (BD Biosciences) and analyzed with FlowJo software (Tree Star) at the INRS-Institut Armand-Frappier Cytometry Facility.

**Flow cytometry and phenotypic analysis.** To characterize gB-specific CD8$^+$ T cells, dispersed spleens or TG (pooled TG; 2 TG at 8 and 14 dpi and 4 TG at 33 dpi) were stained with gB tetramers, followed by cell surface marker staining with anti-CD8$\alpha$, -CD3$\varepsilon$, -CD127, -KLRG-1, -CD44, -CD62L, -PD-1,

or -CD103 as required, and then fixed as described above. To assess TG-resident $CD8^+$ T cells at 36 to 39 dpi, dispersed TG were stained with anti-CD45, -CD8$\alpha$, -CD3$\varepsilon$, and -CD103 and then fixed as described above. To analyze leukocytes within TG and corneas at the indicated times p.i., single-cell suspensions were obtained as described above and treated with unconjugated anti-CD16/CD32 for 15 min at RT prior to surface staining. Neutrophils were identified as $CD45^+$ Gr-$1^{Hi}$ Ly-$6C^{Lo}$, inflammatory monocytes were identified as $CD45^+$ Gr-$1^{Lo\text{-}neg}$ $CD11b^+$ Ly-$6C^{Hi}$, and global monocytes/macrophages were identified as $CD45^+$ Gr-$1^{Lo\text{-}neg}$ $CD11b^+$ Ly-$6C^{Lo\text{-}neg}$.

**BrdU incorporation.** Mice were injected intraperitoneally with 1 mg BrdU (in PBS). Twelve hours later, dispersed spleens or TG were stained for cell surface markers, followed by fixation, permeabilization, and intracellular staining for BrdU following the manufacturer's instructions (BD Biosciences).

**Intracellular cytokine staining and lytic-granule exocytosis.** To assess lytic-granule release, at 8 dpi, single-cell suspensions were prepared from spleens as described above and pulsed with $10^{-6}$ M gB peptide in the presence of FITC-conjugated anti-CD107a MAb and brefeldin A (eBioscience) for 4 h at 37°C and 5% $CO_2$ (51–53). Following stimulation, the cells were stained for surface expression of CD8$\alpha$ and CD3$\varepsilon$, after which they underwent fixation, permeabilization (intracellular fixation and permeabilization buffer; eBioscience), and intracellular staining for IFN-$\gamma$, TNF-$\alpha$, and GrzB.

**Ex vivo reactivation assays.** Following corneal infection of mice and the subsequent establishment of a latent infection, TG were excised and dissociated as described above at the indicated time points (between 36 and 39 dpi). Dissociated cells from individual TG were overlaid on a monolayer of Vero cells. Reactivation for each TG was determined by the appearance of virus-induced cytopathic effect of the Vero cells, which were monitored for 10 days postexplant.

**Statistical analysis.** All statistical analyses were performed with GraphPad Prism software using the Mann-Whitney test; *P* values of less than 0.05 were considered statistically significant. Graphed results are shown as means ± standard errors of the mean (SEM). For *ex vivo* reactivation assays, the chi-squared test was used to determine significant differences ($P < 0.05$).

## ACKNOWLEDGMENTS

We thank the National Institutes of Health Tetramer Core Facility for supplying tetramers. We thank P. P. Pandolfi for the 129/Sv *Dok-1*$^{-/-}$ and *Dok-2*$^{-/-}$ mice.

This work was funded by operating grants from the Canadian Institutes of Health Research to A.P. (MOP-82924) and P.D. (MOP-74445).

## REFERENCES

1. Knipe DM, Howley PM. 2013. Fields virology, 6th ed, vol II. Lippincott Williams and Wilkins, Philadelphia, PA.
2. Fatahzadeh M, Schwartz RA. 2007. Human herpes simplex virus infections: epidemiology, pathogenesis, symptomatology, diagnosis, and management. J Am Acad Dermatol 57:737–763. https://doi.org/10.1016/j.jaad.2007.06.027.
3. Bauer D, Mrzyk S, van Rooijen N, Steuhl KP, Heiligenhaus A. 2000. Macrophage-depletion influences the course of murine HSV-1 keratitis. Curr Eye Res 20:45–53. https://doi.org/10.1076/0271-3683(200001)2011-HFT045.
4. Mott K, Brick DJ, van Rooijen N, Ghiasi H. 2007. Macrophages are important determinants of acute ocular HSV-1 infection in immunized mice. Invest Ophthalmol Vis Sci 48:5605–5615. https://doi.org/10.1167/iovs.07-0894.
5. Kodukula P, Liu T, Rooijen NV, Jager MJ, Hendricks RL. 1999. Macrophage control of herpes simplex virus type 1 replication in the peripheral nervous system. J Immunol 162:2895–2905.
6. Liu T, Tang Q, Hendricks RL. 1996. Inflammatory infiltration of the trigeminal ganglion after herpes simplex virus type 1 corneal infection. J Virol 70:264–271.
7. Ghiasi H, Cai S, Perng GC, Nesburn AB, Wechsler SL. 2000. The role of natural killer cells in protection of mice against death and corneal scarring following ocular HSV-1 infection. Antiviral Res 45:33–45. https://doi.org/10.1016/S0166-3542(99)00075-3.
8. Grubor-Bauk B, Arthur JL, Mayrhofer G. 2008. Importance of NKT cells in resistance to herpes simplex virus, fate of virus-infected neurons, and level of latency in mice. J Virol 82:11073–11083. https://doi.org/10.1128/JVI.00205-08.
9. Tumpey TM, Chen SH, Oakes JE, Lausch RN. 1996. Neutrophil-mediated suppression of virus replication after herpes simplex virus type 1 infection of the murine cornea. J Virol 70:898–904.
10. Sciammas R, Kodukula P, Tang Q, Hendricks RL, Bluestone JA. 1997. T cell receptor-gamma/delta cells protect mice from herpes simplex virus type 1-induced lethal encephalitis. J Exp Med 185:1969–1975. https://doi.org/10.1084/jem.185.11.1969.
11. Ghiasi H, Cai S, Perng GC, Nesburn AB, Wechsler SL. 2000. Both $CD4^+$ and $CD8^+$ T cells are involved in protection against HSV-1 induced corneal scarring. Br J Ophthalmol 84:408–412. https://doi.org/10.1136/bjo.84.4.408.
12. Rajasagi NK, Kassim SH, Kollias CM, Zhao X, Chervenak R, Jennings SR. 2009. $CD4^+$ T cells are required for the priming of $CD8^+$ T cells following infection with herpes simplex virus type 1. J Virol 83:5256–5268. https://doi.org/10.1128/JVI.01997-08.
13. Frank GM, Lepisto AJ, Freeman ML, Sheridan BS, Cherpes TL, Hendricks RL. 2010. Early CD4(+) T cell help prevents partial CD8(+) T cell exhaustion and promotes maintenance of herpes simplex virus 1 latency. J Immunol 184:277–286. https://doi.org/10.4049/jimmunol.0902373.
14. Simmons A, Tscharke DC. 1992. Anti-CD8 impairs clearance of herpes simplex virus from the nervous system: implications for the fate of virally infected neurons. J Exp Med 175:1337–1344. https://doi.org/10.1084/jem.175.5.1337.
15. Wallace ME, Keating R, Heath WR, Carbone FR. 1999. The cytotoxic T-cell response to herpes simplex virus type 1 infection of C57BL/6 mice is almost entirely directed against a single immunodominant determinant. J Virol 73:7619–7626.
16. Wallace ME, Bryden M, Cose SC, Coles RM, Schumacher TN, Brooks A, Carbone FR. 2000. Junctional biases in the naive TCR repertoire control the CTL response to an immunodominant determinant of HSV-1. Immunity 12:547–556. https://doi.org/10.1016/S1074-7613(00)80206-X.
17. Lang A, Nikolich-Zugich J. 2005. Development and migration of protective $CD8^+$ T cells into the nervous system following ocular herpes simplex virus-1 infection. J Immunol 174:2919–2925. https://doi.org/10.4049/jimmunol.174.5.2919.
18. Khanna KM, Bonneau RH, Kinchington PR, Hendricks RL. 2003. Herpes simplex virus-specific memory $CD8^+$ T cells are selectively activated and retained in latently infected sensory ganglia. Immunity 18:593–603. https://doi.org/10.1016/S1074-7613(03)00112-2.
19. Verjans GM, Hintzen RQ, van Dun JM, Poot A, Milikan JC, Laman JD, Langerak AW, Kinchington PR, Osterhaus AD. 2007. Selective retention of herpes simplex virus-specific T cells in latently infected human trigeminal ganglia. Proc Natl Acad Sci U S A 104:3496–3501. https://doi.org/10.1073/pnas.0610847104.

20. Theil D, Derfuss T, Paripovic I, Herberger S, Meinl E, Schueler O, Strupp M, Arbusow V, Brandt T. 2003. Latent herpesvirus infection in human trigeminal ganglia causes chronic immune response. Am J Pathol 163:2179–2184. https://doi.org/10.1016/S0002-9440(10)63575-4.
21. St Leger AJ, Jeon S, Hendricks RL. 2013. Broadening the repertoire of functional herpes simplex virus type 1-specific CD8+ T cells reduces viral reactivation from latency in sensory ganglia. J Immunol 191:2258–2265. https://doi.org/10.4049/jimmunol.1300585.
22. Himmelein S, St Leger AJ, Knickelbein JE, Rowe A, Freeman ML, Hendricks RL. 2011. Circulating herpes simplex type 1 (HSV-1)-specific CD8+ T cells do not access HSV-1 latently infected trigeminal ganglia. Herpesviridae 2:5. https://doi.org/10.1186/2042-4280-2-5.
23. Wakim LM, Woodward-Davis A, Liu R, Hu Y, Villadangos J, Smyth G, Bevan MJ. 2012. The molecular signature of tissue resident memory CD8 T cells isolated from the brain. J Immunol 189:3462–3471. https://doi.org/10.4049/jimmunol.1201305.
24. Liu T, Khanna KM, Chen X, Fink DJ, Hendricks RL. 2000. CD8(+) T cells can block herpes simplex virus type 1 (HSV-1) reactivation from latency in sensory neurons. J Exp Med 191:1459–1466. https://doi.org/10.1084/jem.191.9.1459.
25. Hoshino Y, Pesnicak L, Cohen JI, Straus SE. 2007. Rates of reactivation of latent herpes simplex virus from mouse trigeminal ganglia ex vivo correlate directly with viral load and inversely with number of infiltrating CD8+ T cells. J Virol 81:8157–8164. https://doi.org/10.1128/JVI.00474-07.
26. Janssen E, Zhang W. 2003. Adaptor proteins in lymphocyte activation. Curr Opin Immunol 15:269–276. https://doi.org/10.1016/S0952-7915(03)00044-X.
27. Veillette A. 2004. Specialised adaptors in immune cells. Curr Opin Cell Biol 16:146–155. https://doi.org/10.1016/j.ceb.2004.01.002.
28. Mashima R, Hishida Y, Tezuka T, Yamanashi Y. 2009. The roles of Dok family adapters in immunoreceptor signaling. Immunol Rev 232:273–285. https://doi.org/10.1111/j.1600-065X.2009.00844.x.
29. Shinohara H, Inoue A, Toyama-Sorimachi N, Nagai Y, Yasuda T, Suzuki H, Horai R, Iwakura Y, Yamamoto T, Karasuyama H, Miyake K, Yamanashi Y. 2005. Dok-1 and Dok-2 are negative regulators of lipopolysaccharide-induced signaling. J Exp Med 201:333–339. https://doi.org/10.1084/jem.20041817.
30. Niki M, Di Cristofano A, Zhao M, Honda H, Hirai H, Van Aelst L, Cordon-Cardo C, Pandolfi PP. 2004. Role of Dok-1 and Dok-2 in leukemia suppression. J Exp Med 200:1689–1695. https://doi.org/10.1084/jem.20041306.
31. Yasuda T, Shirakata M, Iwama A, Ishii A, Ebihara Y, Osawa M, Honda K, Shinohara H, Sudo K, Tsuji K, Nakauchi H, Iwakura Y, Hirai H, Oda H, Yamamoto T, Yamanashi Y. 2004. Role of Dok-1 and Dok-2 in myeloid homeostasis and suppression of leukemia. J Exp Med 200:1681–1687. https://doi.org/10.1084/jem.20041247.
32. Mashima R, Honda K, Yang Y, Morita Y, Inoue A, Arimura S, Nishina H, Ema H, Nakauchi H, Seed B, Oda H, Yamanashi Y. 2010. Mice lacking Dok-1, Dok-2, and Dok-3 succumb to aggressive histiocytic sarcoma. Lab Invest 90:1357–1364. https://doi.org/10.1038/labinvest.2010.121.
33. Berger AH, Niki M, Morotti A, Taylor BS, Socci ND, Viale A, Brennan C, Szoke J, Motoi N, Rothman PB, Teruya-Feldstein J, Gerald WL, Ladanyi M, Pandolfi PP. 2010. Identification of DOK genes as lung tumor suppressors. Nat Genet 42:216–223. https://doi.org/10.1038/ng.527.
34. Yasuda T, Bundo K, Hino A, Honda K, Inoue A, Shirakata M, Osawa M, Tamura T, Nariuchi H, Oda H, Yamamoto T, Yamanashi Y. 2007. Dok-1 and Dok-2 are negative regulators of T cell receptor signaling. Int Immunol 19:487–495. https://doi.org/10.1093/intimm/dxm015.
35. Celis-Gutierrez J, Boyron M, Walzer T, Pandolfi PP, Jonjic S, Olive D, Dalod M, Vivier E, Nunes JA. 2014. Dok1 and Dok2 proteins regulate natural killer cell development and function. EMBO J 33:1928–1940. https://doi.org/10.15252/embj.201387404.
36. Coppin E, De Grandis M, Pandolfi PP, Arcangeli ML, Aurrand-Lions M, Nunes JA. 2016. Dok1 and Dok2 proteins regulate cell cycle in hematopoietic stem and progenitor cells. J Immunol 196:4110–4121. https://doi.org/10.4049/jimmunol.1501037.
37. Laroche-Lefebvre C, Yousefi M, Daudelin JF, Charpentier T, Tarrab E, Klinck R, Lamarre A, Labrecque N, Stager S, Duplay P. 2016. Dok-1 and Dok-2 regulate the formation of memory CD8+ T cells. J Immunol 197:3618–3627. https://doi.org/10.4049/jimmunol.1600385.
38. Banerjee K, Biswas PS, Rouse BT. 2005. Elucidating the protective and pathologic T cell species in the virus-induced corneal immunoinflammatory condition herpetic stromal keratitis. J Leukoc Biol 77:24–32.
39. Banerjee K, Rouse BT. 2007. Immunopathological aspects of HSV infection, p 642–655. *In* Arvin A, Campadelli-Fiume G, Mocarski E, Moore PS, Roizman B, Whitley R, Yamanishi K (ed), Human herpesviruses: biology, therapy, and immunoprophylaxis. Cambridge University Press, Cambridge, United Kingdom.
40. Sheridan BS, Cherpes TL, Urban J, Kalinski P, Hendricks RL. 2009. Reevaluating the CD8 T-cell response to herpes simplex virus type 1: involvement of CD8 T cells reactive to subdominant epitopes. J Virol 83:2237–2245. https://doi.org/10.1128/JVI.01699-08.
41. Jeon S, St Leger AJ, Cherpes TL, Sheridan BS, Hendricks RL. 2013. PD-L1/B7-H1 regulates the survival but not the function of CD8+ T cells in herpes simplex virus type 1 latently infected trigeminal ganglia. J Immunol 190:6277–6286. https://doi.org/10.4049/jimmunol.1300582.
42. Chentoufi AA, Kritzer E, Tran MV, Dasgupta G, Lim CH, Yu DC, Afifi RE, Jiang X, Carpenter D, Osorio N, Hsiang C, Nesburn AB, Wechsler SL, BenMohamed L. 2011. The herpes simplex virus 1 latency-associated transcript promotes functional exhaustion of virus-specific CD8+ T cells in latently infected trigeminal ganglia: a novel immune evasion mechanism. J Virol 85:9127–9138. https://doi.org/10.1128/JVI.00587-11.
43. Srivastava R, Khan AA, Garg S, Syed SA, Furness JN, Vahed H, Pham T, Yu HT, Nesburn AB, BenMohamed L. 9 November 2016. Human asymptomatic epitopes identified from the herpes simplex virus tegument protein VP13/14 (UL47) preferentially recall polyfunctional effector memory CD44high CD62Llow CD8+ TEM cells and protect humanized HLA-A*02:01 transgenic mice against ocular herpesvirus infection. J Virol https://doi.org/10.1128/JVI.01793-16.
44. Khan AA, Srivastava R, Spencer D, Garg S, Fremgen D, Vahed H, Lopes PP, Pham TT, Hewett C, Kuang J, Ong N, Huang L, Scarfone VM, Nesburn AB, Wechsler SL, BenMohamed L. 2015. Phenotypic and functional characterization of herpes simplex virus glycoprotein B epitope-specific effector and memory CD8+ T cells from symptomatic and asymptomatic individuals with ocular herpes. J Virol 89:3776–3792. https://doi.org/10.1128/JVI.03419-14.
45. Alvarez de Celis H, Gomez CP, Descoteaux A, Duplay P. 2015. Dok proteins are recruited to the phagosome and degraded in a GP63-dependent manner during Leishmania major infection. Microbes Infect 17:285–294. https://doi.org/10.1016/j.micinf.2014.12.011.
46. St Leger AJ, Peters B, Sidney J, Sette A, Hendricks RL. 2011. Defining the herpes simplex virus-specific CD8+ T cell repertoire in C57BL/6 mice. J Immunol 186:3927–3933. https://doi.org/10.4049/jimmunol.1003735.
47. Mott KR, Allen SJ, Zandian M, Konda B, Sharifi BG, Jones C, Wechsler SL, Town T, Ghiasi H. 2014. CD8alpha dendritic cells drive establishment of HSV-1 latency. PLoS One 9:e93444. https://doi.org/10.1371/journal.pone.0093444.
48. Mott KR, Gate D, Matundan HH, Ghiasi YN, Town T, Ghiasi H. 29 April 2016. CD8+ T cells play a bystander role in HSV-1 latently infected mice. J Virol https://doi.org/10.1128/jvi.00255-16.
49. Lymberopoulos MH, Pearson A. 2007. Involvement of UL24 in herpes-simplex-virus-1-induced dispersal of nucleolin. Virology 363:397–409. https://doi.org/10.1016/j.virol.2007.01.028.
50. Leiva-Torres GA, Rochette PA, Pearson A. 2010. Differential importance of highly conserved residues in UL24 for herpes simplex virus 1 replication in vivo and reactivation. J Gen Virol 91:1109–1116. https://doi.org/10.1099/vir.0.017921-0.
51. Betts MR, Brenchley JM, Price DA, De Rosa SC, Douek DC, Roederer M, Koup RA. 2003. Sensitive and viable identification of antigen-specific CD8+ T cells by a flow cytometric assay for degranulation. J Immunol Methods 281:65–78. https://doi.org/10.1016/S0022-1759(03)00265-5.
52. Betts MR, Koup RA. 2004. Detection of T-cell degranulation: CD107a and b. Methods Cell Biol 75:497–512. https://doi.org/10.1016/S0091-679X(04)75020-7.
53. Wolint P, Betts MR, Koup RA, Oxenius A. 2004. Immediate cytotoxicity but not degranulation distinguishes effector and memory subsets of CD8+ T cells. J Exp Med 199:925–936. https://doi.org/10.1084/jem.20031799.